

# Probability, Causality and False Alarms using Correlations Between Strong Earthquakes and NOAA High Energy Electron Bursts

Cristiano Fidani<sup>1,2</sup>

<sup>(1)</sup> Central Italy Electromagnetic Network, Via Fosso del Passo 6, 63900 Fermo, Italy

<sup>(2)</sup> Osservatorio Sismico “Andrea Bina”, Borgo XX Giugno, 06121 Perugia, Italy

Article history: received October 5, 2018; accepted April 10, 2019

## Abstract

A proposal for testing the feasibility of strong earthquake forecasting from space, using on board high energy particle detectors of existing NOAA polar satellites, is given. Previously, exceptional increases of particle fluxes prior to and after the largest quakes that struck the Indonesian and the Philippine areas were recently recognised utilising NOAA-15 particle telescopes. A statistically significant correlation between electron bursts of 30 – 100 keV and large seismic events was calculated in previous publications, occurring 2 – 3 hours between seismic events having  $M \geq 6$  and electron bursts. The 2 – 3 hour correlation supports the hypothesis that there is a physical link between ionospheric charged particle motions at around 2,000 km and seismic activities when earthquake depths are less than 200 km. Taking into account the corresponding electron drift periods and the detector energy corrections, the time interval of a possible physical interaction between high energy electrons of the inner radiation belts and the earth's crust of the future earthquake epicentre has been reduced to about 4 – 6.5 hours. A causal model is proposed for the entire process. Cross-correlation coefficients are calculated starting from the previously obtained correlations, so that a probability of earthquake forecasting corresponding to the 2 – 3 hour peak can be evaluated. Based on these results, false alarms can be reduced in an experiment where such probability is used for one year of average seismic and electron loss detections. Finally, an experiment is proposed here, which is currently feasible using ongoing NOAA satellites and USA West Coast antennas to test the forecasting.

Keywords: NOAA satellites, Electron bursts, Statistical correlations, Earthquake forecasting, False alarms.

---

## 1. Introduction

Over the last twenty years, many strong earthquakes (EQs) have occurred worldwide which have produced many deaths and massive damage costing billions of euros and dollars even though several of these affected areas had had EQ-resistant buildings. These events were useful for observing different physical parameters

## Cristiano Fidani

from space, with the goal of testing some selected deviations from what is usually observed. Previous specific results on EQs and ionospheric particles correlations had regarded different space missions, such as the MIR orbital station, METEOR-3 and GAMMA [Aleksandrin et al., 2003], SAMPEX satellite [Sgrigna et al., 2005], and the NOAA-15 satellite [Rothkaehl et al., 2006]. The NOAA-15 particle database, which has been collecting data since 1998, was systematically studied for its particle bursts in connection with global strong seismic activity in periods of weak solar activity [Fidani, 2015]. This analysis showed that exceptional increases of electron fluxes, hereinafter called electron bursts (EBs), prior to the largest quakes which had struck the defined Indonesian and Philippine areas, were statistically correlated with seismic events. EBs at each NOAA satellite semi-orbit, referred to as extended EBs, were analysed in order to distinguish their correlations with seismic activities from seasonal variations belonging to particles associated with geomagnetic activity. When analysing 30 – 100 keV precipitating electrons and EQ with epicentre projections at altitudes greater than 1,400 km using invariant coordinates [McIlwain, 1966], significant correlations appeared. Specifically, a 2 – 3 hour electron precipitation excess was detected prior to large events in Indonesia and the Philippines, suggesting a 4 – 10 hour early warning of strong EQs influencing the ionosphere [Fidani, 2015]. Therefore, an experiment was proposed to verify the feasibility of strong EQs forecasting from space using existing NOAA POES [Fidani, 2016a, 2016b]. After that, the same calculus was tested also for contiguous EBs definition, with EBs occurring many times in a single semi-orbit, which produced a super Poissonian statistic for the correlation distribution [Fidani 2018a]. Finally, a possibility to use the correlation in the calculus of a conditional EQ probability given an EB detection was suggested [Fidani 2016b, 2017a, 2018a, 2018b].

Ionospheric disturbances linked to seismic activity were first observed around the time of the great Alaska EQ [Davies et al., 1965] on March 28, 1964. Satellites measurements [Larkina et al., 1983] have recognised the potential of this research, which provided medium and far field viewing points of lithosphere phenomena with respect to the EQ influence sizes. Several of the particle detectors used in solar studies from low earth orbit satellites have been used to investigate electron precipitation in connection with strong EQs during time periods with weak geomagnetic variations [Aleksandrin et al., 2003; Sgrigna et al., 2005]. These studies were based on data coming from satellite missions lasting only a few months or collected over a few months with equal attitude data, therein providing weak evidence for correlations. The NOAA-15 satellite, which has been collecting data since 1998, permitted for a particle database with almost constant conditions of detector efficiency and orbit stability [Davis 2007]. To evaluate perturbations from normal undisturbed conditions, the NOAA-15 particle analysis included mainly satellite positions under the inner radiation belts [Fidani, 2015]. The inner radiation belt has been reported to be significantly affected by geomagnetic activity [Millan and Thorne, 2007], and the particle analysis also included a comparison with the solar wind velocity [Vassiliadis, 2008]. In fact, magnetic storms can induce sudden electron flux enhancements of more than one order of magnitude near  $L = 2$  [Alexandrin et al., 2008], and NOAA particle bursts auto-correlations have indicated a clear Sun influence also during geomagnetically quiet periods [Fidani et al., 2012].

Starting from the above results, periods with very low geomagnetic activity were only included in these analyses, using variable thresholds with seasonal and multi years periods. Moreover, correlation calculus was carried out using main shocks only, as EQ clustering highly condition correlation events [Fidani et al., 2010]. Correlation calculuses in past publications were obtained making specific selections in electron parameters. These parameters are used here to test for a causal association among EQ-EB interaction, EB detection, EQ occurrence, and EB absorption. This model considers the degradation of NOAA electron detectors which was not included in the past publications, and it is shown to reduce the time interval when the EQ-EB interaction takes place. The significant correlations that were reported in past publications were calculated considering EQ and EB events as unitary events. Being so, these correlations were only positively defined and need to be redefined to consider both positive and negative values. It is made here by taking into account past calculated correlations and the total number of considered hours, EQ events, and EB events. Based on this, a conditional probability is evaluated to respond to the question if EQ forecasting should be possible starting from the correlation results. The number of false alarms was also estimated for one year of EQ forecasting. Finally, the feasibility of an EQ forecasting experiment was tested using operative NOAA satellite equipment and facilities.

## 2. NOAA EBs, strong EQs and geomagnetic activity data sources

The comparison of different types of data required to prepare them homogeneously. The preparation of NOAA data consisted of the storage of all binary files into Ntuples [Couet et al., 1998], where the time step was 8 seconds. From July 1, 1998, to December 31, 2014, binary data were downloaded from NOAA (<http://www.ngdc.noaa.gov/stp/satellite/poes/dataaccess.html>) and examined to exclude uncorrected instrument operations through their corresponding flags. The electron counting rates were corrected for proton contamination [Rodger et al., 2010] using the software downloaded from the Virtual Radiation Belt Observatory (<http://virbo.org/POES#Processing>).

In order to include the geomagnetic and extraterrestrial influences on the particle fluctuations, the counting rates data were associated with daily averages of the geomagnetic Ap index and SID (<http://www.aavso.org/solar-sids>), as well as three-hour averages of the Ap index (<ftp://ftp.ngdc.noaa.gov/STP/GEOMAGNETICDATA/APSTAR/apindex>). The counting rate data exclusions from the correlation analysis occurred when geomagnetic indexes overcame thresholds, which were calculated by annual and 11-year Sun particle modulations [Fidani, 2015]. As counting rate fluctuations originating in the magnetosphere also occur in sub-storm activity, the validity of the selected days with very weak geomagnetic activity was tested by controlling that Dst variations ([http://wdc.kugi.kyoto-u.ac.jp/dst\\_final/index.html](http://wdc.kugi.kyoto-u.ac.jp/dst_final/index.html)) were less than 30 nT. *B*-field and McIlwain parameter were re-evaluated on the NOAA-15 orbit utilising the latest [Thébault et al., 2015] International Geomagnetic Reference Field (IGRF-12) model (<http://www.ngdc.noaa.gov/IAGA/vmod/igrf.html>), to include recent model corrections of past years, as well as height variations along the satellite orbits.

To correlate seismic activity with NOAA data, a Ntuple was created which contains EQ data including event time, location, magnitude, and depth. The values of the corresponding *L*-shells of the EQ epicentres projected to different altitudes were also calculated utilising the same methodology used for particles and included in the Ntuples. This was done to determine where the possible physical link works between EQ and EB. The EQ list was downloaded from the EQ Centre of United States Geological Survey (USGS) at <http://neic.usgs.gov/neis/epic/epic.html>, and has been adjusted to eliminate foreshocks and aftershocks, see Figure 1.

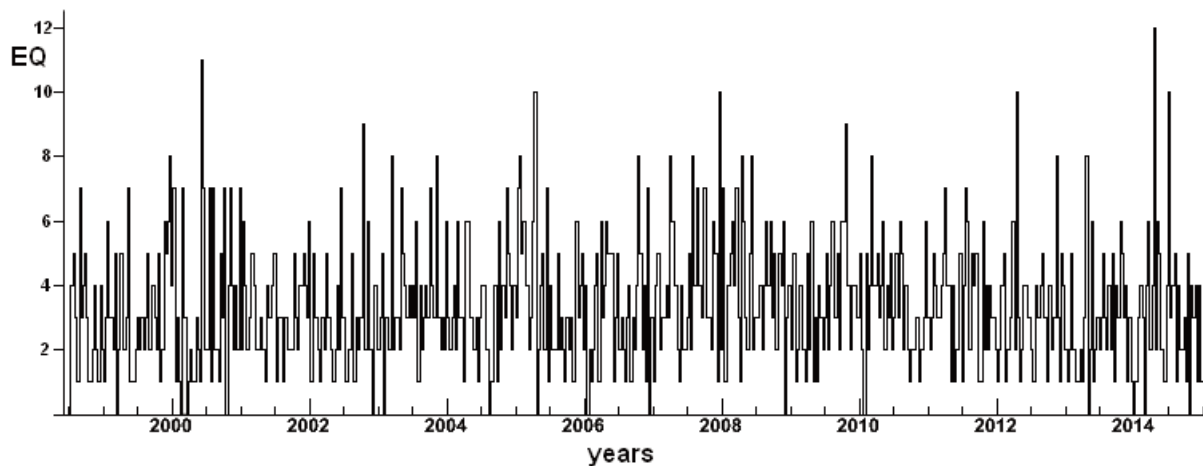


**Figure 1.** The  $M \geq 6$  maishock distribution over the 16.5 years of this study, it is reported as a sum of mainshocks recorded worldwide every 10 days.

Starting from daily averages in counting rates, a condition for which electron counting rate fluctuations were not likely due to statistical fluctuations with a probability larger than 99% was defined as EB [Fidani et al., 2008] for discrete intervals of *L*-shell, pitch angle, and geomagnetic field *B* values. The charged particle motions were strongly variable along the satellite orbit and the use of this coordinate system obtained more stable results, compared to

studies using orbital coordinates. Moreover, EBs were restricted by selecting electrons coming out from steadily trapped conditions, which means that electrons were disturbed in their motion at some positions. Such conditions were applied to collect a set of EBs from July 1998 to December 2014, see Figure 2.

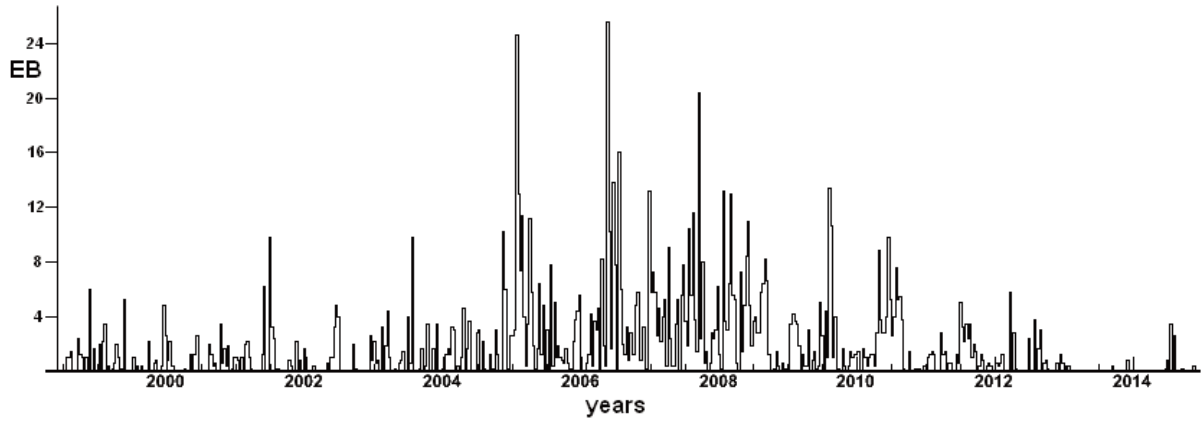


**Figure 2.** Precipitating EBs in the drift loss cone recorded every 10 days over 16.5 years of NOAA-15 detection in a low  $L$ -shell interval for electron energy from 30 keV to 100 keV with the zenith telescope.

### 3. Correlation between NOAA EBs and strong EQs

Following the procedure described in past publications [Fidani, 2015] correlations were obtained by defining  $L_{EQ}$ , so to evidence some positions in the ionosphere starting with the EQ geographical positions projected along the vertical at fixed altitudes. The corresponding  $L$ -shells were assigned by the same geomagnetic software used for counting rates and therefore for EBs. Defining  $L$ -shells relative to EBs as  $L_{EB}$ , the subsets of EQs and EBs satisfying the condition

$$|L_{EQ} - L_{EB}| \leq 0.1, \quad (1)$$

were further analysed. The differences  $T_{EQ} - T_{EB}$ , between the EQ time  $T_{EQ}$  and the EB time  $T_{EB}$ , only for those seismic events and particle precipitations {EQ;EB} which satisfied (1) were collected in a histogram where, in other words, for every time interval of one hour relative to  $T_{EQ} - T_{EB}$ , was calculated

$$\sum_{\{EQ;EB\}} (EQ \times EB), \quad (2)$$

where EQ and EB can assume only 0 and 1 values. Being that EQ and EB are digital events, the histogram (2) obtained by  $T_{EQ} - T_{EB}$  is a positive correlation of binary sequences or bitstreams. The binary correlation coefficient (2) was calculated for a set of time differences of  $\pm 72$  hours. It was repeated at 39 altitudes of EQ epicentre projections, by estimating  $L_{EQ}$  at each altitude from  $-600$  km up to  $3,200$  km, compared to the sea level, in increments of  $100$  km.

Several correlation peaks appeared from the first electron energy channels corresponding to  $30 - 100$  keV detected by the vertical telescope [Fidani, 2015]. Whereas, correlation peaks did not appear from  $100 - 300$  keV and  $300 - 2,700$  keV electron energy channels utilising vertical telescope or from any electron energy channels utilising horizontal or omnidirectional telescopes. Furthermore, no correlation peaks up until now have appeared from similar NOAA-15 proton analyses. The same algorithm was applied to the particle databases of all other NOAA polar satellites, but no correlation peaks were observed from the first electron energy channels, nor from any other energy channels or particle types (Fidani 2015). The dawn-dusk orbit of NOAA-15 was the only one different from the other NOAA POES orbits, which were all characterised by day/night.

## Probability, Causality and False Alarms of Earthquakes by NOAA Electron Bursts

A correlation plot of EBs with 30 – 100 keV energy is shown in Figure 3 and was obtained by projecting EQ positions at 1,800 km. The plot in Figure 3 depicts the statistical correlation calculated over more than 16 years of data collecting the time difference between strong EQ occurrence and EB detection  $T_{EQ} - T_{EB}$  from -24 to 24 hours. The distribution shapes and average values were compared with standard deviations of correlation events, evidencing a Poissonian distribution. The peak at 2 – 3 hours started to be significant when considering EQ projections above 1,400 km altitudes [Fidani, 2015] and maximised with EQ projections of 2,200 km. Correlations were maximised by using EQ magnitudes  $M \geq 6$ . Pitch angle restrictions required that the particles be precipitating, meaning that their values were mostly in the loss cone. Specifically, particles in these EBs were concentrated in intervals around  $65^\circ$  and  $135^\circ$ . Results in Figure 3 were obtained by removing pitch angles from the intervals with  $0^\circ \leq \alpha \leq 30^\circ$ ,  $80^\circ \leq \alpha \leq 120^\circ$  and  $160^\circ \leq \alpha \leq 360^\circ$ . The depths of analysed EQs were lower than 200 km, that is they had to be close to the surface. The 2 – 3 hour result is identical to that obtained when using many contiguous EBs for each orbit, which produced super-Poissonian distributions for correlation events [Fidani, 2018a].

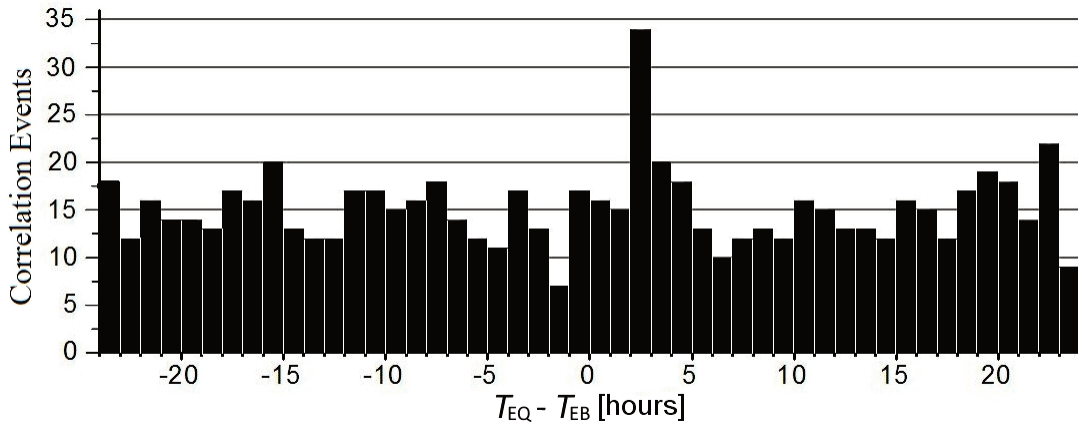


**Figure 3.** The 48 hours correlation between EQs and EBs previously published using 16.5 years of NOAA-15 data.

### 4. A causal model of EB motions and satellite detections

A statistical correlation between two observables is not sufficient to prove a physical link between them. Thus, the research for a physical model able to link earth crust dynamic of EQs and the dynamic of EBs in the ionosphere is necessary. To do this, a possibility is to start with the correlation results, which means to start with the selected parameters of both EQs and EBs, and then to apply the physical laws of charged particle electrodynamic and satellite orbital dynamic to proceed. Beginning this analysis with correlations, it is noteworthy that epicentre locations having EQs correlated with EBs were in both the Indonesian and the Philippine Regions, having  $90^\circ$  to  $150^\circ$  longitudes, with few events in South America [Fidani, 2015]. Whereas, the NOAA detection area was located high offshore of the USA and the South America West Coasts, between a longitude between  $200^\circ$  and  $280^\circ$ . These different electron positions could have been associated in a causal way, due to the fact that electrons drift eastwards and the EQ positions were located west of the EB detection positions. In turn, if any kind of disturbances above the EQ epicentres occurred, it would have perturbed electrons motions and thus EBs would have been detected sometime after.

From the Van Allen Belts electrodynamics, electron drift periods depend on energy by [Walt, 1994]:

$$T_d = \frac{1.05}{E(\text{MeV})L} \frac{1}{1+0.43 \sin \alpha_{eq}}, \quad (3)$$

where  $\langle \alpha_{eq} \rangle$  is the equatorial pitch angle which is near  $90^\circ$ . For energies of 30 keV and 100 keV the periods result being

21 to 6 hours covering the whole earth longitudes, respectively. The correlated electrons belonged to the low  $L$ -shell range of  $1.15 < L < 1.35$ , like those obtained for correlations of EBs. However, a recent evaluation of particle detectors on board NOAA satellites established that the minimum detected energy reached 60 keV a few years after the launch of the satellites [Yando et al., 2011]. On the other hand, 2 – 3 hour correlations had a major contribution years after the NOAA-15 launch. This was because the first years were characterised by high geomagnetic disturbances and there were few useful days, see Figure 4. In fact in this picture, times of EQs occurrence and local times of EB detections by NOAA-15 dawn-dusk orbit which contributed to the correlations are anti-correlated with respect to the solar activity during the entire period. Thus, the electron energy interval of 60 keV to 100 keV was considered for the correlations and a correspondent period of between 10.5 to 6 hours was necessary to cover all of the longitudes, respectively. The electrons which produced the correlations crossed the satellite vertical detectors in the drift loss cone high offshore the USA and the South America West Coasts around an average of  $120^\circ$  eastwards, about 2 – 3 hours before the EQ times. Being so, it was calculated that a time interval of 2 – 3.5 hours was necessary for 60 – 100 keV electrons to drift  $120^\circ$ . So, if the disturbances which caused electron precipitations from inner radiation belts occurred above the EQ epicentres in the ionosphere, they anticipated the EQ times by 4 – 6.5 hours, which is a reduced interval with respect to those previously calculated of 4 – 10 hours [Fidani, 2015]. Similar observations in time advance disturbances have been made for other physical variables detected at EQ longitudes [Anagnostopoulos et al., 2012].

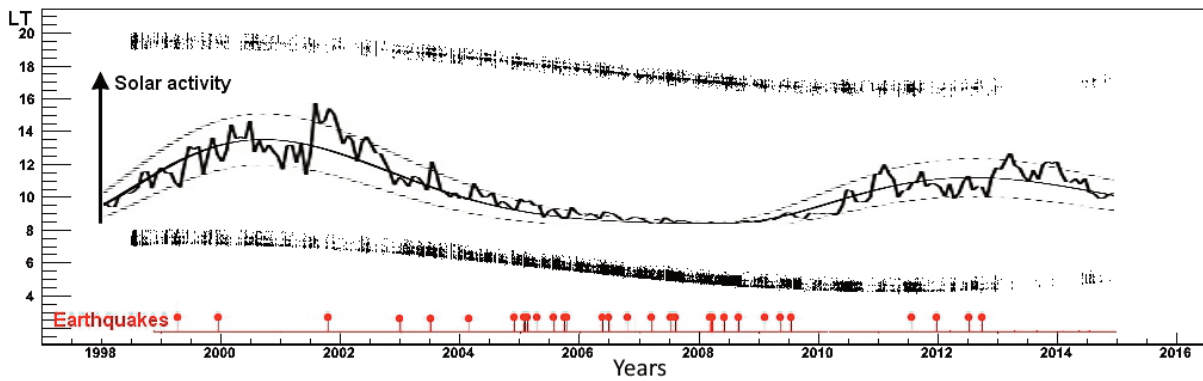


**Figure 4.** The local time of the NOAA-15 satellite during the more than 16 years of this study. The point density estimates the probability of detecting EBs which are probably not due to solar activity; solar activity is depicted in the centre of this plot. Strong EQs which were anticipated from 2 – 3 hours of EB precipitations are indicated by red points. Most of the EQs were included in the correlation, as most days and EBs were included in the analysis during the solar minimum.

The low  $L$ -shell range of  $1.15 < L < 1.35$  obtained for correlated EBs provides information about the altitude where the disturbances could have occurred. In fact, electron  $L$ -shells for the correlations were near the  $L$ -shells associated to the EQs, these were calculated starting from the EQ altitude projections. Being so, the deduced EQs  $L$ -shell range of  $1.05 < L < 1.45$ , due to (1) corresponded to altitude projections ranging between 1,400 and 2,800 km. These altitudes are the altitudes of disturbed electrons above the EQ epicentres, therefore they can be thought of as the altitudes where disturbances worked if they had occurred in the places nearer to the EQ epicentres. Given this, the physical link between earth crust and electron motion must have been able to cover at least 2,000 km. In a recent experiment activated during strong seismic activity in Central Italy, magnetic detectors were able to record strong magnetic pulses hours before the mainshock [Orsini and Fidani, 2017]. This observation was made by at least one station belonging to the Central Italy Electromagnetic Network [Fidani, 2017b]. The magnetic observation was of a such a high intensity at about 100 km from the EQ epicentre, that it was thought to be able to reach the ionosphere with a significant intensity [Orsini and Fidani, 2018]. Furthermore, its frequency of 1 Hz to 10 Hz, were similar to the observations made in other countries [Scoville et al., 2015; Li et al., 2016], and resulted being in resonance with the bouncing motion of electrons at detected energies by NOAA satellites [Walt, 1994]. These results support the hypothesis that there could be an electron pitch angle disturbances due to magnetic ULF signals from the ground [Galper et al., 1995].

## Probability, Causality and False Alarms of Earthquakes by NOAA Electron Bursts

Finally, the information from the pitch angles that electrons of detected EBs are precipitating electrons means that their bouncing point altitudes were lowered during disturbances at EQ epicentre longitudes. Lower mirror point altitudes above Indonesia and the Philippines were not sufficient to cross the NOAA-15 satellite which has an altitude of about 800 km. However, given the eastward drift of the electrons and the asymmetry of the geomagnetic field, the crossing between the electron motions and NOAA orbits was possible high offshore of the USA and the South America West Coasts. In fact, at these longitudes, the electron mirror point altitudes have to have gradually touched the satellite altitude and went lower. Further drifting eastwards, electron mirror point altitudes have to have gone lower and lower up to down under 100 km, which is the atmospheric altitude. Doing so, they were absorbed in correspondence of the South Atlantic Anomaly, about 2 hours later the crossing of NOAA-15 satellites where a part of them was detected. In this sense, they were called precipitating electrons, as electrons were absorbed in South Atlantic Anomaly, not above the EQ epicentres nor where NOAA detected them but having some hours of life after they were disturbed. The whole process is described in Figure 5.

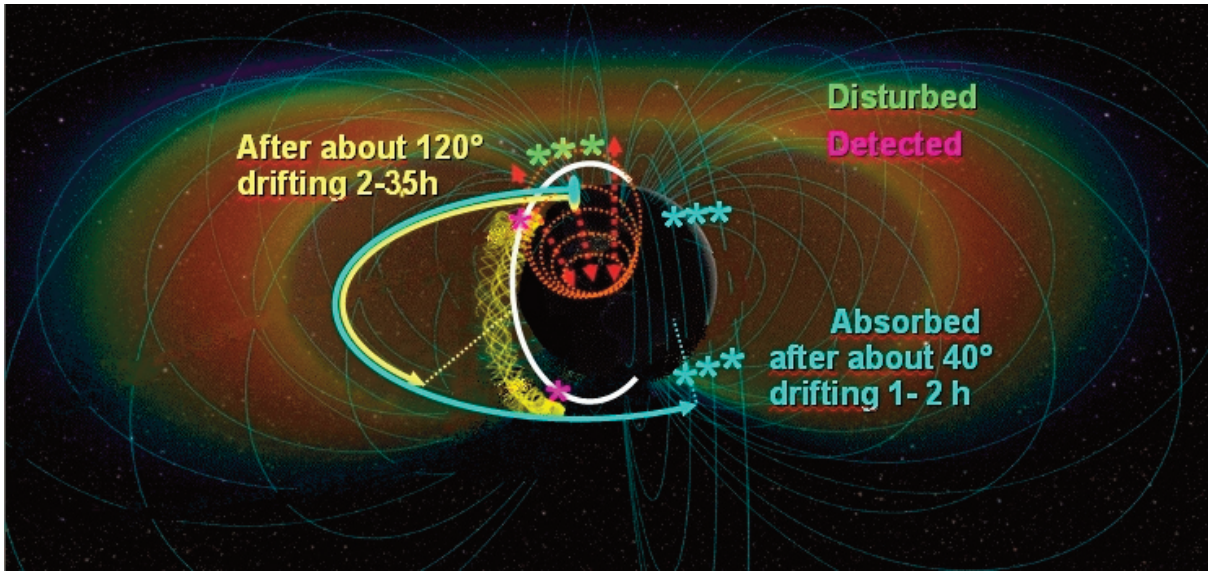


**Figure 5.** A possible physical model to causally connect EQ and EB events. Dimensions of the Inner Van Allen Belts are not in scale to obtain a clearer representation of EB dynamics. The image was modified from the NASA animation downloaded at <https://www.nasa.gov>

## 5. EQ probability and false alarms in a forecasting experiment

If such a causal connection exists, a question needs are raised: could the 2 – 3 hour correlation be used for future strong EQ forecasting? The response to this seems to be affirmative for what concerns the probability of a strong EQ over the next 2 – 3 hours in Indonesia or the Philippines. This probability can be calculated throughout the relationship between the covariance and cross correlation [Billingsley, 1995] applied to EQ and EB unitary events

$$\text{corr}(EQ,EB) = \text{cov}(EQ,EB) / \sqrt{P(EQ)[1-P(EQ)]P(EB)[1-P(EB)]}, \quad (4)$$

with  $\text{cov}(EQ,EB) = [P(EQ \cap EB) - P(EQ)P(EB)]$ , and where  $P(EQ)$  and  $P(EB)$  are the independent probabilities of EQs and EBs occurrence, respectively. Then the joint probability is

$$P(EQ \cap EB) = P(EQ)P(EB) + \text{corr}(EQ,EB) \sqrt{P(EQ)[1-P(EQ)]P(EB)[1-P(EB)]}, \quad (5)$$

and the conditional probability  $P(EQ|EB) = P(EQ \cap EB) / P(EB)$  is

$$P(EQ|EB) = P(EQ) + \text{corr}(EQ,EB) \sqrt{P(EQ)[1-P(EQ)]} [1-P(EB)] / P(EB). \quad (6)$$

Which means that, if a correlation exists between EQs and EBs, and the time difference is chosen to be that of correlations between EQ and EB events, the probability of a strong EQ is increased of a term proportional to the correlation.

However, the correlation term appearing in relations (4), (5), and (6) is not the same as the binary correlation defined in (2); in fact, it is the cross-correlation coefficient which can be both positive and negative. To find a link using (2) to obtain (4), the following expression can be used for the cross-correlation coefficient

$$corr(EQ,EB) = (E[EQ,EB] - E[EQ]E[EB]) / \sqrt{(E[EQ^2] - E^2[EQ])(E[EB^2] - E^2[EB])}, \quad (7)$$

where  $E[]$  is the expectation. Being for binary events  $E[EQ] = E[EQ^2] = P(EQ)$ ,  $E[EB] = E[EB^2] = P(EB)$  and the relation (4) can be rewritten in terms of covariance throughout the population formula

$$cov(EQ,EB) = [N_h \sum_{\{EQ,EB\}} (EQ \times EB) - N_{EQ} N_{EB}] / N_h^2, \quad (8)$$

where  $N_{EQ}$  and  $N_{EB}$  are the numbers of EQ and EB which participated in the correlation, respectively; while  $N_h$  is the number of total hours considered for the correlation. Being so, the probabilities of single events are  $P(EQ) = N_{EQ}/N_h$  and  $P(EB) = N_{EB}/N_h$ . To evaluate them it can be considered that the observed correlation was calculated only when the geomagnetic activity was very low. It corresponds to only 996 days over 16.5 years, equal to 23,906 hours. Furthermore, the NOAA satellite moves in a synchronous orbit to the Sun's position, going intermittently high offshore the USA and South American West Coasts only for about half a day's time, the effective hours of detection reducing to  $N_h = 11,953$  hours. During the same time intervals, there were detected  $N_{EB} = 1,051$  EBs, so defining a  $P(EB) = 0.088$ , in other words, the average of one EB every 11.4 hours. A total of 2023 mainshocks struck the earth surface in 16.5 years, which correspond to  $N_{EQ} = 167$  EQs and about 122 EQs/year, defining a  $P(EQ) = 0.014$ , in other words, an average of one main shock with  $M \geq 6$  every 3 days. The cross-correlation coefficients were recalculated using (8) and the cross-correlation plot is shown in Figure 6, which now assumes both positive and negative values. Based on (8), the expression (6) can be simplified in

$$P(EQ|EB) = \sum_{\{EQ,EB\}} (EQ \times EB) / N_{EB}, \quad (9)$$

and tell that the previous calculated correlation is proportional to the conditional probability. Using the 2 – 3 hour correlation peak equal to 34 of (2), the conditional EQ forecasting probability can be calculated in  $P(EQ|EB) = 0.032$ , and referring it to (6) it describes a net increase due to a correlation of 0.018, which is 128% above  $P(EQ)$  value.

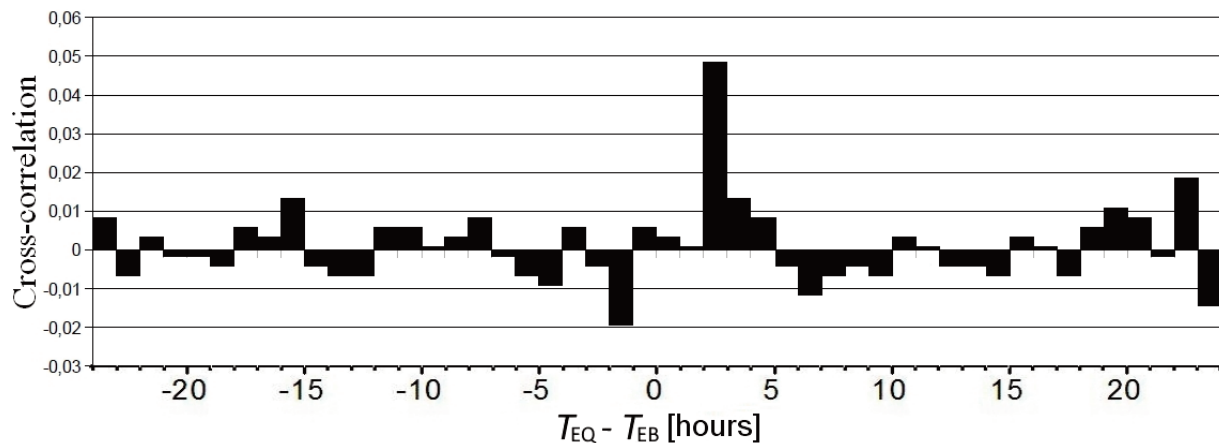


**Figure 6.** The EQ – EB Pearson correlation coefficients calculated starting from the correlation reported in Figure 3, included the number of total hours, EQs and EBs in this analysis.

## Probability, Causality and False Alarms of Earthquakes by NOAA Electron Bursts

Concerning the average number of false alarms over one year of EB and EQ activities, it can be calculated by the average number of EBs over one year, which is equal to 63. Then, as  $P(\text{EQ}|\text{EB}) = 0.032$ , it is necessary for about 30 attempts to forecast one EQ given an EB detection. It means that two EQs in one year are on average forecasted with 63 EBs. However, calculating the average global number of EQs that in one year are linkable to EBs, (which means to consider the part of 122 EQs multiplied by 1/6 of the time while there was low geomagnetic activity and by half of the time when the satellite was able to detect EBs), it resulted in being about 10 EQs. So, about two EQs would have been anticipated by two EBs, while 8 EQs would not have been anticipated by any EBs, which means that 61 EBs would not have been followed by EQs, leading to 61 false alarms. Even if restricted to Indonesian and Philippine EQs the average number of EBs to consider in one year is always 63. The recalculated conditional probability  $P(\text{EQ}|\text{EB}) = 0.029$  corresponds to the necessity of 34 attempts to forecast one EQ given an EB detection, and near two EQs in one year are forecasted on average. A total of 600 mainshocks struck the Indonesian and the Philippine Regions in 16.5 years, which correspond to about 36 EQ/years, defining a  $P(\text{EQ}) = 0.004$ , in other words, one main shock with  $M \geq 6$  for 10 days on average. The average number of EQs that in one year are linkable to Ebs, in this case, results in being around 3 EQs. This means, still about two EQs would have been anticipated by two EBs, while one EQ would not have been anticipated by any EBs, which means that 61 EBs would not have been followed by EQs, leading still to 61 false alarms. Nevertheless, being  $P(\text{EQ}) = 0,014$  for the global case, about 140 false alarms would be necessary before two EQs are forecast, and  $P(\text{EQ}) = 0,004$  being the case for the Indonesian and Philippine Regions, about 500 false alarms would be necessary before two EQs are forecast both without the use of satellites. Therefore, in spite of a high number of false alarms, it was reduced by 2.3 times for the global seismic activity and by 8.3 times for the Indonesian and the Philippines seismic activity thanks to the analysis of NOAA particle data. Moreover, forecasted EQs were 20% for the global and 66% for the Indonesian and Philippines Regions of EQs occurring during the useful time of 11,953 hours.

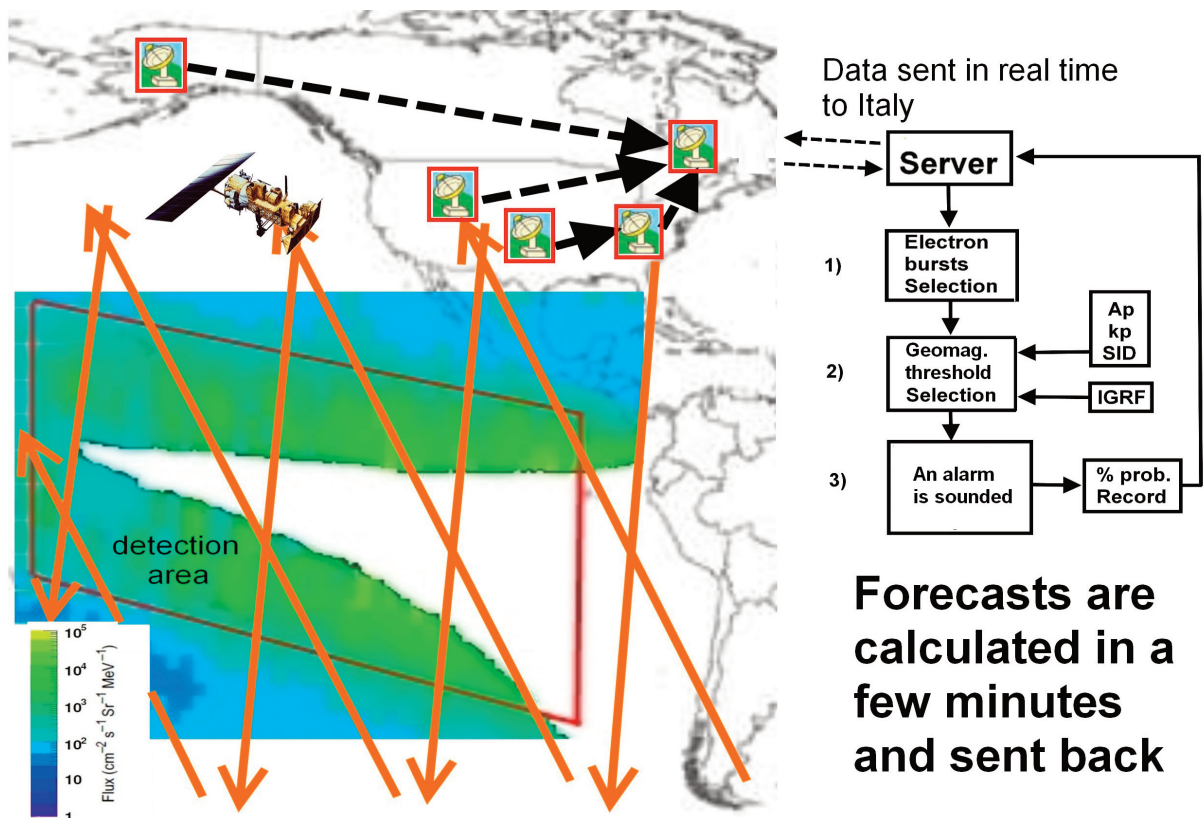


**Figure 7.** A real-life experiment using the NOAA-15 satellite and the USA West Coast antennas. Semi-orbits which cover the region high offshore the USA and South American West Coasts over 24 hours are indicated with red arrows. Downloads from the ends of downward semi-orbits are difficult due to their distance from the antennas, however, these downloads are possible at one hour later at the beginning of the next semi-orbit.

A major problem in utilizing the proposed method in a real-life experiment is that it is difficult to obtain the necessary particle data right after they have been detected. Specifically, given that the correlation peak between EQs and EBs occurs at the 2 – 3 hour time interval, electron detections have to be downloaded from the NOAA satellite no later than one hour after they have been collected. This is not always possible at every position because, currently, antennas for downloading data do not cover the entire ionosphere. However, the NOAA-15 satellite did not detect EBs correlated with EQs at all longitudes. As reported in past publications and in the above described model, EBs that contributed to correlations were detected high offshore over the USA and the South American West Coasts, between 200° and 280° longitude. That being so, the four antennas operating along the USA West Coast should be able to download NOAA data early enough, see Figure 7. NOAA POES are polar satellites, and antennas operating along the USA West Coast seem to be optimal for downloading data from NOAA traveling from the Southern to Northern hemisphere, as their positions are North-West near the end of NOAA semi-orbits high offshore over the USA West Coast. Being so, the possibility to download upcoming NOAA data a few minutes after they have been detected is almost certain. It would however be more difficult to download data from the NOAA moving North to South. In fact, when satellites are flying towards the South Pole they are more distant from the USA West Coast antennas at the end of descending semi-orbits. Given that the NOAA satellite period is about 100 minutes, they are again visible by USA West Coast antennas after about an hour, at the beginning of the next semi-orbit. Then, the main requirement for using the above method in a real-life experiment using NOAA satellites seems to be satisfied. After downloading, the data can then be sent directly to any server in the world for processing.

The software for processing these data must follow the lines described in previous publications on correlations, in order to set off an alarm. This software should be able to: 1) verify if EBs are detected; if not present, there will be no alarms; if present, it will be required to 2) verify if the geomagnetic disturbances are under the thresholds described in past publications; if not then no alarms are set off; if the disturbances are under 3) an alarm is sounded throughout Indonesia and Philippines for a full hour starting from the successive hour for a strong EQ occurring in Indonesia and the Philippines, and 4) the global seismic network verifies the EQ occurrence labelling the alarm as either false or correct. The forecasting 3) is sent back from the server to NASA in a few minutes. Step 1) is realised by calculating averages in electron counting rates over the previous 24 hours and verifying if the detected variations are exceptional increases in counting rates. This first step requires access to the previous 24 hour data which is completely feasible. Step 2) is realised by verifying that real-time geomagnetic activity is under geomagnetic index thresholds. This second step requires the access of near real time geomagnetic indexes such as  $A_p$ ,  $K_p$ , and  $D_{st}$ , with about one hour of delay. It is very difficult to obtain in one hour with the worldwide network of geomagnetic observatories, as it releases geomagnetic data with usually one day of delay. However, a forecasting service for geomagnetic activity and indexes is working, which could be used for this scope. Steps 3) and 4) are realisable in a completely automatic way and simply require high PC computation performances and a reliable web connection. Finally, after two hours the alarm is ended.

## 6. Conclusions

A physical model is essential for proving that a statistical correlation corresponds to a phenomenological link. By using 16.5 years of NOAA particle data, a statistically significant correlation between EBs and large EQs of 2 – 3 hours before mainshocks in Indonesia and the Philippines has been reported in past publications. The parameters used to obtain the correlation and the electrodynamics of electrons in the Van Allen Belts suggest a possible causal link. Based on the drift period (3), and hypothesizing that a physical interaction between electrons and EQs occurred in the ionosphere, above the epicentre of Indonesia and the Philippines, the physical interaction was calculated to anticipate EQ times by 4 – 6.5 hours, a considerably reduced interval with respect to the previously published results.

A method and an experiment are proposed for EQ forecasting, both are based on an evaluation of Indonesian and Philippine large EQ probabilities with EB detections by the NOAA-15 satellite. Here, the conditional probability  $P(EQ|EB)$  increased with respect to the random probability  $P(EQ)$  of one term proportional to the cross-correlation coefficient. However, the correlation obtained in past works was not in the correct form to be used for the conditional probability. The cross-correlation coefficients were obtained starting from the old correlation calculus through the population formula. A possible EQ forecasting experiment showed that the probability of EQ forecasting in Indonesia and the Philippines given an EB detection by the NOAA-15 satellite can be increased by over 100%.

## Probability, Causality and False Alarms of Earthquakes by NOAA Electron Bursts

However, the number of false alarms for a year of average EQ and EB activities remains high and equal to 61, while there would be two correctly forecasted EQs either for global or Indonesian and Philippine seismic activities. In spite of a high number of false alarms, it was reduced by 2.3 times with 20% of useful EQs forecasted for the global seismic activity and it was reduced by 8.3 times with 66% of useful EQs forecasted for the Indonesian and Philippine seismic activities, thanks to the analysis of NOAA particle data. Finally, a type of experiment for EQ forecasting in Indonesia and The Philippines is feasible using the NOAA-15 satellite, given the presence of the USA West Coast antennas.

**Acknowledgments.** I would like to thank the “Consulta delle Fondazioni delle Casse di Risparmio Umbre”, the “A. Bina” seismic observatory, and SARA Electronics Instruments for supporting this study. Also, I would like to express my thanks to Craig J. Rodger and Janet Green from NOAA for their useful codes to subtract the proton contamination of electron channels.

## References

- Aleksandrin, S. Yu., Galper, A. M., Grishantzeva, L. A., Koldashov, S. V., Maslennikov, L. V., Murashov, A. M., Picozza, P., Sgrigna, V., and Voronov, S. A. (2003). High-energy charged particle bursts in the near-Earth space as earthquake precursors. *Annales Geophysicae*, 21, 597–602.
- Anagnostopoulos, G. C., Vassiliadis, E., Pulinet, S. (2012). Characteristics of flux-time profiles, 20 temporal evolution, and spatial distribution of radiation-belt electron precipitation bursts in the upper ionosphere before great and giant earthquakes. *Ann. Geophys. – Italy* 55, 21–36.
- Asikainen, T. and K. Mursula (2008). Energetic electron flux behavior at low L-shells and its relation to the South Atlantic Anomaly, *J. Atmosph Solar-Terr. Phys.*, 70, 532–538.
- Billingsley, P. (1995). *Probability and Measure* (3rd ed.). New York: John Wiley and Sons.
- Couet, O. and M. Goossens, (1998). *HBOOK Statistical Analysis and Histogramming Reference Manual*; Information Technology Division, CERN: Geneva, Switzerland.
- Davies, K. and D. M. Baker (1965). Ionospheric effects observed around the time of the Alaskan earthquake of March 28, *J. Geophys. Res.*, 70, 2251–2253.
- Davis, G. (2007). History of the NOAA satellite program. *J. Appl. Remote Sensing* 1, 012504.
- Evans, D. S. and M. S Greer (2004). *Polar Orbiting Environmental Satellite Space Environment Monitor – 2: Instrument Descriptions and Archive Data Documentation*. NOAA Technical Memorandum January, version 1.4, 155.
- Fidani, C. and R. Battiston (2008). Analysis of NOAA particle data and correlations to seismic activity. *Nat. Haz. Earth Syst. Sci.*, 8, 1277–1291.
- Fidani, C., R. Battiston and W. J. Burger (2010). A study of the correlation between earthquakes and NOAA satellite energetic particle bursts. *Remote Sens.*, 2, 2170–2184.
- Fidani, C., R. Battiston, W. J. Burger, and I. Conti (2012). A study of NOAA particle flux sensitivity to solar activity and strategies to search for correlations among satellite data and earthquake phenomena, *Int. J. Remote Sens.*, 33, 15, 4796-4814.
- Fidani, C. (2015). Particle precipitation prior to large earthquakes of both the Sumatra and Philippine Regions: A statistical analysis, *J. Asian Earth Sci.*, 114, 384–392.
- Fidani, C. (2016a). Forecasting Strong Earthquakes in Indonesia and Philippines from Space, *International Beacon Satellite Symposium BSS-2016*, Trieste, Italy.
- Fidani, C. (2016b). Strong Earthquakes in Indonesia and Philippines warned in advance from Space, *35<sup>th</sup> General Assembly of the European Seismological Commission ESC-2016*, 4-10 September, Trieste, Italy.
- Fidani, C. (2017a). Probability and strong earthquakes from low earth orbit satellites, *36<sup>th</sup> GNGTS*, Trieste. 311-314, Nov. 14-16.
- Fidani, C. (2017b). Ten Years of the Central Italy Electromagnetic Network (CIEN) Continuous Monitoring, *Open J. Earthquake Res.*, 6, 73-88.
- Fidani, C. (2018a). Improving Earthquake Forecasting by Correlations Between Strong Earthquakes and NOAA Electron Bursts, *TAO*, 29, 2, 117-130.

## Cristiano Fidani

- Fidani, C. (2018b). Correlations between VAB electron loss detected by NOAA and strong seismic activity used to improve forecasting of  $M \geq 6$  earthquakes, EMSEV2018, Potenza. 124-127, Sep. 17-21.
- Galper, A. M., S. V. Koldashov, and S. A. Voronov, (1995). High energy particle flux variations as earthquake predictors. *Adv. Space Res.*, 15, 11, 131–134.
- Larkina, V. I., V. V. Migulin A. V., Nalivaiko, N. I. Gershenzon, M. B. Gokhberg, V. A. Liperovsky, S. L. Shalimov (1983). Observations of VLF emission, related with seismic activity on the Interkosmos-19 satellite, *Geomagnetism and Aeronomy*, 23, 684–687.
- Li, M., H. Tan and M. Cao (2016). Ionospheric influence on the seismo-telluric current related to electromagnetic signals observed before the Wenchuan  $M_S$  8.0 earthquake, *Solid Earth*, 7, 1405–1415.
- McIlwain, C. E. (1966). Magnetic coordinates, *Space Sci. Rev.* 5, 585–598.
- Millan, R. M., Thorne, R. M. (2007). Review of radiation belt relativistic electron losses, *J. Atmos. Solar-Terrestrial Phys.* 69, 362–377.
- Orsini, M. and C. Fidani (2017). Magnetic perturbations observed around the October 30, 2016 Norcia earthquake,  $M = 6.5$ , 36th GNGTS, Trieste. 316-318 Nov. 14-16.
- Orsini, M. and C. Fidani (2018). Modelling magnetic pulse swarms that anticipated the 2016 Norcia, and 2017 Capitignano, Central Italy earthquakes, EMSEV2018, Potenza. 87-89, Sep. 17-21.
- Rodger, C. J., M. A., Clilverd, J. Green and M.M. Lam (2010). Use of POES SEM-2 observations to examine radiation belt dynamics and energetic electron precipitation in to the atmosphere. *J. Geophys. Res.*, 115, A04202.
- Rothkaehl, H., R. Bucik. and K. Kudela. (2006). Ionospheric plasma response to the seismic activity. *Phys. Chem. Earth*, 31, 473–481.
- Sgrigna, V., L. Carota, L. Conti, M. Corsi, A. M., Galper, S. V. Koldashov, A. M., Murashov, P. Picozza, R. Scrimaglio, L. Stagni (2005). Correlations between earthquakes and anomalous particle bursts from SAMPEX/PET satellite observations. *J. of Atmos. Solar-Terrestrial Phys.*, 6, 15, 1448-1462.
- Scoville, J., J. Heraud, and F. Freund (2015). Pre-earthquake magnetic pulses. *Nat. Hazards Earth Syst. Sci.*, 15, 1873–1880.
- Thébault, E., C. Finlay, C. D Beggan, P. Alken, J. Aubert, O. Barrois, F. Bertrand, T. Bondar, A. Boness, L. Brocco, E. Canet, A. Chambodut, A. Chulliat, P. Coïsson, F. Civet, A. Du, A. Fournier, I. Fratter, N. Gillet, B. Hamilton, M. Hamoudi. G. Hulot, T. Jager, M. Korte, W. Kuang, X. Lalanne, B. Langlais, J.-M. Léger, V. Lesur, F. J. Lowes, S. Macmillan, M. Mandea, M., C. Manoj, S. Maus, N. Olsen, V. Petrov, V. Ridley, M. Rother, T. J Sabaka, D. Saturnino, R. Schachtschneider, O. Sirol, A. Tangborn, A. Thomson, L. Tøffner-Clausen, P. Vigneron, I. Wardinsk and T. Zvereva (2015). International Geomagnetic Reference Field: the 12th generation, *Earth, Planets and Space*, 67:79.
- Vassiliadis, D. (2008). Response of the radiation belt electron flux to the solar wind velocity: parameterization by radial distance and energy. *J. Atmos. Solar- Terrestrial Phys.* 70 (14), 1810–1828.
- Walt, M. (1994). Introduction to Geomagnetically Trapped Radiation. Cambridge University, Cambridge, p. 168.
- Yando, K., R. M. Millan, J. C. Green, D. S. Evans (2011). A Monte Carlo simulation of the NOAA POES medium energy proton and electron detector instrument. *J. Geophys. Res.* 116, A10231.

**\*CORRESPONDING AUTHOR: Cristiano FIDANI**

Central Italy Electromagnetic Network,  
Via Fosso del Passo 6, 63900 Fermo, Italy and  
Osservatorio Sismico “Andrea Bina”,  
Borgo XX Giugno, 06121 Perugia, Italy,  
e-mail: c.fidani@virgilio.it

© 2020 the Istituto Nazionale di Geofisica e Vulcanologia.

All rights reserved